

H. Aydın MD<sup>1</sup>  
N. Aydın Oktay MD<sup>1</sup>  
B. Hekimoglu MD<sup>1</sup>

## Visualization of the 12<sup>th</sup> Cranial Nerve with MRI: Value of Balanced Fast-Field Echo and 3D-Drive Sequences Among the T2 TSE Post-Contrast T1 Sequences

**Background/Objective:** Our aim was to optimize the most effective MR imaging sequence for visualization of the 12th cranial nerve (hypoglossal nerve) through its cisternal course.

**Patients and Methods:** We applied balanced fast-field echo (B-FFE), 3D-T2 weighted Driven Equilibrium RF Reset Pulse (DRIVE), T2 weighted 2D TSE and post-contrast T1 weighted sequences and tried to find out the best sequence for the perfect visualization of the 12th cranial nerve. One-hundred patients without any hypoglossal nerve paralysis were examined via these sequences. Imaging analysis was graded as follows: certain visualization of nerves (score 2), partially visualized nerves (score 1), non-visualized nerves (score 0).

**Results:** The hypoglossal nerve was visualized exactly in only eight cases and partially depicted in only six cases with the post-contrast T1 series. In B-FFE sequence; 56% of the nerves were properly seen and 8% of the nerves were partially identified, using T2 weighted DRIVE sequences; 30% of the nerves were clearly visualized, the nerves were partially depicted in 15 patients. Regarding the T2 weighted TSE sequence, 15% of the nerves were certainly depicted and in seven patients the nerves were partially depicted.

**Conclusion:** The most diagnostic sequence for the exact visualization of the cisternal course of hypoglossal nerve is B-FFE revealing a 64% visualization rate for the cisternal parts (112 exactly, 16 partially). T2W DRIVE sequence is shown to be more diagnostic than the T2W TSE for visualization of the cisternal part of the hypoglossal nerve.

Key words: MR Imaging, Twelfth Cranial Nerve, 3D-MR Imaging, MRI Scans, Drive

### Introduction

**H**ypoglossal nerve fibers originate from the hypoglossal nucleus that is located in the para-median aspect of the base of the fourth ventricle, medially to the dorsal nucleus of vagus nerve. The anterior column of the spinal cord extends caudally to the nucleus and produces a slight bulging into the fourth ventricle, named the hypoglossal eminence.<sup>1,2</sup> Axons intercourse through the medullary tegmentum from the anterior side, pass over the medial aspect of the inferior olivary complex and exit as multiple nerve roots in the preolivary sulcus through the pyramid and olive.<sup>1-3</sup>

The nerve roots converge, course ventrally and exit from the cranium through the hypoglossal canal, which is situated in the posteromedial aspect of the jugular foramen.<sup>1,2,4</sup>

The hypoglossal nerve can be divided into extracranial and intracranial parts; the intracranial part comprises the cisternal and the intracanalicular portions.<sup>1,4</sup> The cisternal segment extends through the premedullary cistern and consists of the rootlets and the roots of the hypoglossal nerve.<sup>2-4</sup> The hypoglossal nerve

I. Department of Radiodiagnostic,  
Dışkapı Yıldırım Beyazıt Research Hos-  
pital, Ankara, Turkey.

Corresponding Author:  
Hassan Aydın  
Address: Department of Radiodiagnos-  
tic, Dışkapı Yıldırım Beyazıt Research  
Hospital, Ankara, Turkey  
Tel: +90053 2348 4530  
Fax: +90031 2322 0006  
E-mail: dr.hasanaydin@hotmail.com

Received September 19, 2009;  
Accepted after revision March 7, 2010.

Iran J Radiol 2010;7(2):71-77

runs with the ninth, tenth and eleventh nerves at the level of the mastoid tip where it curves anteriorly to enter the digastric triangle and divides into its branches.<sup>1,4</sup> An important prediction is that the twelfth nerve first travels inferiorly to the level of the hyoid before ascending to the tongue.<sup>1,2,4</sup> Except for the palatoglossus, the hypoglossal nerve supplies all the intrinsic and extrinsic muscles of the tongue.<sup>1,4</sup> The vasculature of the cisternal segment of the hypoglossal nerve comes from the anterolateral and the lateral medullary arteries arising from the perforating and pontomedullary branches of the basilar artery.<sup>2,4</sup>

MR imaging reveals a detailed anatomic evaluation of the cranial nerves; their courses, important sides for their passage and their pathology. With the accurate development of MRI technology, newer 2D-3D heavily T2 weighted sequences with high spatial resolution have been applied such as 3D-CISS (three-dimensional constructive interference in steady state), 3D-MP-RAGE (three-dimensional magnetization-prepared rapid gradient-echo), 3D-FIESTA (three-dimensional fast imaging employing steady-state acquisition).<sup>5-8</sup> Balanced fast-field echo (B-FFE) and 3D-T2 weighted Driven equilibrium RF Reset Pulse (DRIVE) sequences can also supply strong T2 weighted good MR-cisterno-graphic images and may be performed to visualize cranial nerves nuclei or root entry zones.<sup>5-9</sup>

In this research, we planned to define the most efficient sequence for evaluation and visualization of the hypoglossal nerve. For 100 patients we applied B-FFE, 3D-T2W DRIVE, T2W TSE and post-contrast T1W sequences; consequently, we tried to optimize the best sequence for depiction of the 12th cranial nerve.

## Patients and Methods

One-hundred patients with a total of 200 nerves on both sides without hypoglossal nerve paralysis were included in this research. This study was performed in the department of Radiology, Ankara Dışkapı Yıldırım Beyazıt Research Hospital, MR imaging unit.

The criteria for hypoglossal nerve dysfunction include tongue fasciculations, paralysis, discomfort in swallowing and sensori-neural loss in all parts of the tongue. None of the patients involved in this study

had such complaints.

All patients were referred to our department by ear, nose and throat clinicians with temporal MR imaging requests. The patients involved in this research were older than 18 years old. The exclusion criteria were claustrophobic patients, patients with cardiac pacemakers, patients with metallic implants in their bodies and extremities and patients who were unwilling to be involved in the research.

From July to December 2008, 47 males and 53 females in the age range of 14 to 74 years (mean, 50 years) were recruited. Informed consent was obtained before entering the study.

All MRI sections were performed with 1.5 T Philips Nova Dual HP MRI scanner (16 channel Achiva Master, Eindhoven, Netherlands) with a 33 mT/min maximum gradient strength and a 180 mT/ms slew rate, using a standard head coil. We obtained MR imaging using B-FFE, T2W 3D-DRIVE, T2W 3D-TSE and post-contrast T1W sequences. For the post-contrast series, contrast agent 0.1-0.2 mmol/kg gadolinium-DTPA, Magnevist (Schering) or Omniscan (Nycomed) were administered.

The parameters of all MR imaging sequences are demonstrated in Table 1.

## Image Analysis

Analysis of the data obtained from all sequences was based on the original transverse 2D or 3D images with slice thicknesses between 1-2 mm. An 8-year-experienced neuroradiologist evaluated the images for the visualization of hypoglossal nerve, as its rootlets converged anteriorly and exited the skull through the bony hypoglossal canal, just medial to the jugular foramen. Consequently, it was graded and scored as: 1-Certainly identified nerves (score 2, nerves properly visualized on both sides), 2-Probably identified nerves (score 1, nerves partially depicted on both sides or properly visualized on only one side), 3-Unidentified nerves on both sides (score 0). Statistical analysis was performed using the Pearson chi-square test applied upon the SPSS 11.5 (SPSS Inc, Chicago-IL). P value less than 0.05 was considered statistically significant.

All images obtained in the mentioned sequences were handled and processed under the Philips-Achiva View Form Work-station. The MPR refor-

matted images of the 12th cranial nerve in all sequences were also analyzed in this work-station.

The confounding elements in the depiction of hypoglossal nerve are as follows: bilateral flocculonodular lobes of the cerebellum mixed with hypoglossal nerves in post-contrast series due to low spatial resolution, blood vessels near the hypoglossal canal that have close relationship or contact with the nerve roots, antero-lateral and lateral medullary veins, transverse medullary veins, hypoglossal arteries, anterior medullary segment of vertebral arteries, posterior inferior cerebellar artery (PICA) might be confused with 12th cranial nerves, especially in the DRIVE and T2W FSE sequences,<sup>2,3</sup> the hypoglossal nerve and the trochlear nerve had the smallest diameters throughout the cranial nerves;<sup>5,7,10</sup> therefore, adjacent soft tissue, clival adipose tissue and bony fragments could easily interfere with the 12th cranial nerve via the partial volume effect of MR imaging, especially in post-contrast series and FSE sequences.

## Results

We identified 112 nerves on both sides (56%) with score 2 (certainly visualized) (Figs. 1-2) and 16 nerves (8%) with score 1 (partially depicted) by performing B-FFE sequence. Seventy-two hypoglossal nerves on both sides were not visualized with this sequence

(score 0) (Table 2).

In hypoglossal nerve visualization with the T2W-DRIVE sequence, 60 nerves (30%) were properly seen on both sides with a score of 2 (Figs. 3-4) and 30 nerves (15%) were depicted with a score of 1. One-hundred ten nerves on both sides (55%) were not identified via this sequence (score 0) (Table 2).

Using the T2W TSE sequence, 30 hypoglossal nerves (15%) were certainly identified (score 2) (Figs. 5-6), 14 nerves on both sides (7%) were partly identified (score 1), 156 hypoglossal nerves (78%) were not identified (score 0) (Table 2).

When we performed post-contrast T1W sequences, 16 hypoglossal nerves (8%) were certainly identified (score 2) (Fig. 7), 12 nerves on both sides (6%) were partially identified (score 1) and 172 of 200 nerves (86%) were not identified (score 0) (Table 2) (Fig. 8).

Altogether, the hypoglossal nerve was mostly visualized by B-FFE sequence (56% totally, 8% partially identified).

B-FFE scores have significant statistical differences from the results of T2-DRIVE, T2W-TSE and post-contrast T1W sequences with regard to the visualization of hypoglossal nerve ( $p < 0.001$ ). T2-DRIVE sequence results have also definite statistical differences from the scores of T2W-TSE and post-contrast T1W sequences for the identification of hypoglossal nerve ( $p < 0.001$ ). Only T2W-TSE and post-contrast T1W

**Table 1.** Parameters of the Sequences

	B-FFE	T2W 3D-DRIVE	T2W 2D-TSE	Post-Contrast T1W
TR\TE	7.1\3.5 ms	1500\250	3000\120	400\10
Flip angle	50	90	90	90
Matrix	308*320	256*256	168*256	128*256
Field of view (cm)	18*25	13	14.8*17.5	14.8*17.5
Reconstruction field of view(%)	83	100	124	123
NSA-NEX	3	2	2	3
Slice thickness (mm)	1.0	1.4	2.0	2.0
Number of partitions	40	30	12	12
Scan time (min.)	2.03	1.23	1.24	1.44
TSE Factor	-	74	17	3

**Table 2.** The Scores and Percentages of Hypoglossal Nerve Visualization in Each Sequence

Sequences		n (%)	Results			Total
			Not-Identified	Partially Seen	Clearly Visualized	
Sequences	B-FFE	n (%)	72 (36%)	16 (8%)	112 (56%)	200 (100%)
	T2W DRIVE	n (%)	110 (55%)	30 (15%)	60 (30%)	200 (100%)
	T2W TSE	n (%)	156 (78%)	14 (7%)	30 (15%)	200 (100%)
	Post-Contrast T1W	n (%)	172 (86%)	12 (6%)	16 (8%)	200 (100%)
Total		n (%)	510 (64%)	72 (9%)	218 (27%)	800 (100%)

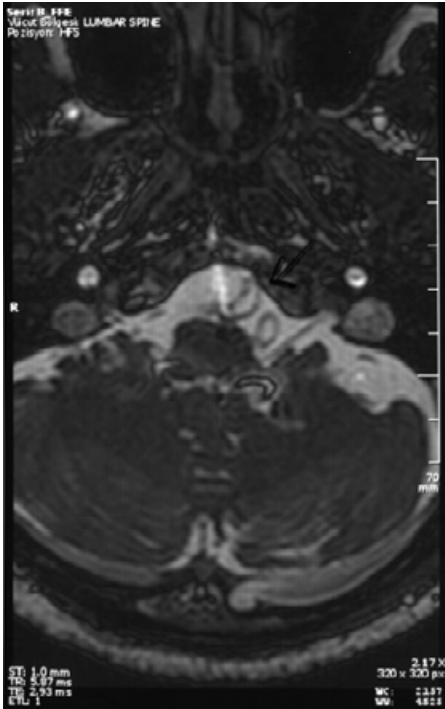


**Fig. 1.** Temporal MRI, axial B-FFE sequence in a 27-year-old man. The left hypoglossal nerve is clearly seen.

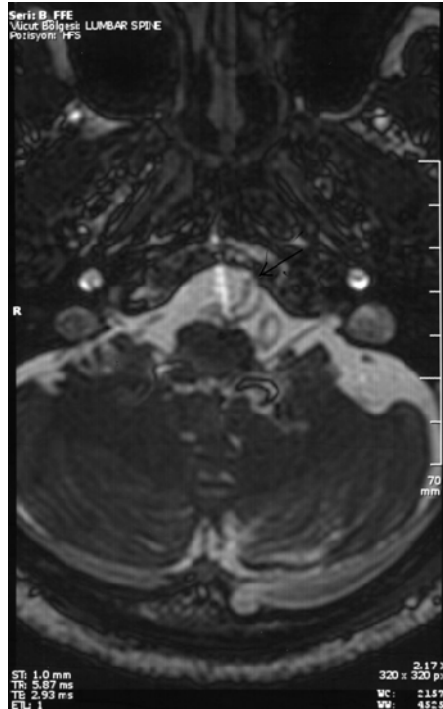


**Fig. 2.** Temporal MRI, axial B-FFE sequence in a 52-year-old woman. Certain identification of the left hypoglossal nerve.

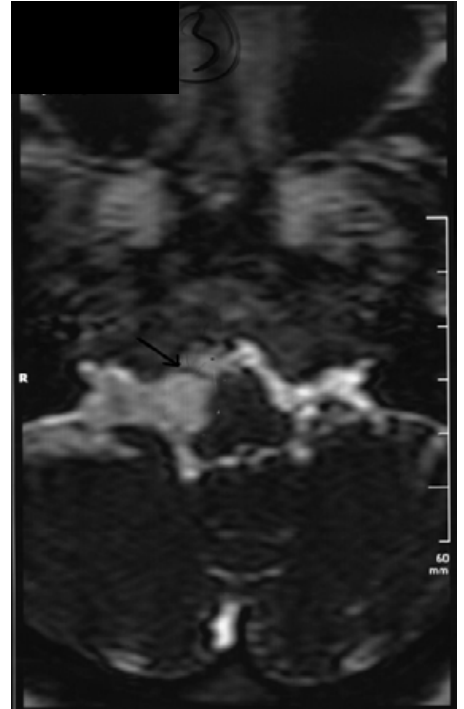


**Fig. 3.** Axial T2W-3D Drive sequence in the temporal MRI of a 32-year-old man. The right hypoglossal nerve is certainly visualized.

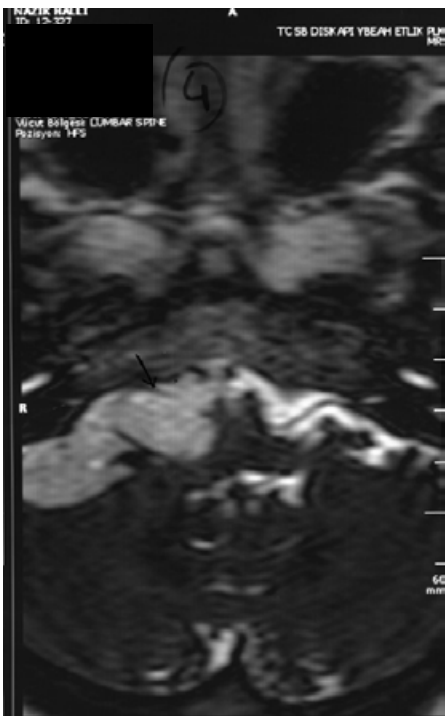


**Fig. 5.** Axial T2W-TSE sequence in a 30-year-old man. Certainly visualized hypoglossal nerves on both sides.



**Fig. 6.** Axial T2W-TSE sequence in a 20-year-old woman. Clearly identified left hypoglossal nerve.

**Fig. 4.** Temporal MRI, axial T2W-3D Drive sequence of a 22-year-old woman. The right hypoglossal nerve is clearly seen in this sequence.

sequences have similar results and their scores showed no significant statistical differences in the depiction of 12<sup>th</sup> cranial nerve (p=0.074).

The intra-observer variability for the determination of 12<sup>th</sup> cranial nerve has significant statistical differences between all these four different sequences

(p<0.001). There was no inter-observer variability as all the images were interpreted by the same radiologist.

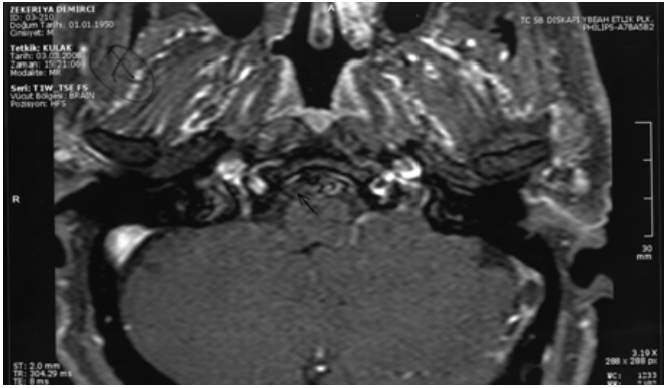


**Fig. 7.** Axial post-contrast T1W sequence in a 35-year-old man. Certainly visualized right hypoglossal nerve is seen in this sequence.

## Discussion

The motor neurons within the hypoglossal nucleus give rise to the axons that course between the medial lemniscus and the pyramidal bundles located medially and the inferior olivary complex situated laterally.<sup>1-4</sup> The axons leave the medulla through the preolivary sulcus as the primary rootlets of the hypoglossal nerve.<sup>2-4</sup> These rootlets form the secondary and the tertiary rootlets afterwards, called the definite roots of the hypoglossal nerve.<sup>1,2,4</sup>

They course at the level of the caudal two thirds of the ponto-medullary bifurcation, just caudal to the olive, and they extend dorsally through the lateral side of the premedullary cistern.<sup>2,3</sup>

The rostral and caudal trunks are formed by the definite roots of the hypoglossal nerve; three trunks or a single trunk is rarely formed.<sup>1-4</sup> Both trunks then enter the hypoglossal canal and form a single nerve

trunk after leaving the bony canal.<sup>2-4</sup> The cisternal course of the hypoglossal nerve is in close relationship with the adjacent vessels such as the anterior medullary segment of the vertebral artery, PICA, lateral anterior medullary vein and the transverse medullary veins.<sup>2</sup>

The pathological classification for the hypoglossal nerve dysfunction is divided into supra-nuclear (central), nuclear (medullary) and the infra-nuclear parts.<sup>1,3,4</sup> Supra-nuclear hypoglossal paralysis is most commonly secondary to cerebral infarcts, multiple sclerosis, encephalitis and pseudobulbar palsy. Nuclear type paralysis is extremely rare.<sup>1,3</sup>

The long infra-nuclear course of the hypoglossal nerve from its origin to the termination in the sublingual space allows a variety of pathologies.<sup>1-4</sup>

The cisternal part of the nerve might be affected in a vertebrobasilar aneurysm or dolichoectasia, skull base neoplasms, basal skull fractures or fractures of the occipital condyle, basal meningitis or subarachnoid hemorrhages.<sup>1,3</sup> Primary tumors of the hypoglossal nerve are very rare but could include schwannomas.<sup>1,4</sup> Malignancies within the nasopharynx, oropharynx and sublingual spaces might also invade the hypoglossal canal and the peripheral aspect of the hypoglossal nerve.<sup>1,3</sup> Hypoglossal nerve palsy has also been reported after neck radiation, during or after the deep neck infections and odontogenic abscesses.<sup>1,4</sup>

As its high spatial resolution and contrast advantages, MR imaging is the gold standard to visualize the cisternal portion of the hypoglossal nerve and the canal. However, newer MR sequences and MR cis-

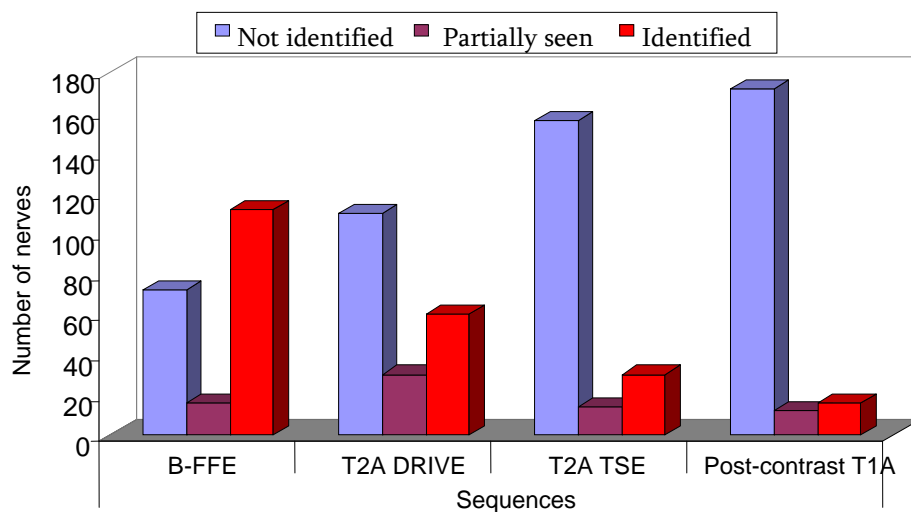


**Fig. 8.** Graph showing the number of not identified, partially seen and identified nerves, depicted in each sequence.

ternography could easily show the anatomic and pathologic courses of the nerve roots with the vessels and dura mater.<sup>5,7,10</sup>

With the routine T1 and T2 weighted sequences, it was really difficult to show the nerve regularly and properly because a) The diameter of the hypoglossal nerve was about 1.3-1.6 mm, b) The hypoglossal nerve fibers course near the vessels of similar caliber and in their course have close relationship with the passing neighbor vessels.<sup>5,7,10</sup>

To overcome all these problems and to depict the 12th cranial nerve properly, heavily T2 weighted sequences are important due to their high sensitivity in the detection of cranial nerve nuclei or root entry zones.<sup>5,7-9,11</sup> By performing heavily T2W sequences with high spatial resolution, hypoglossal nerve with all its course and the hypoglossal canal could be detected more precisely.<sup>5,7,10</sup>

Recently, MR imaging sequences like Steady State Free Precession (SSFP) and DRIVE techniques are generally performed.<sup>5,7-11</sup> SSFP sequences are basically and practically gradient echo sequences; B-FFE, B-TFE, True Fast imaging short period (FISP) and FIESTA are the commercial names of the most unique sequences.<sup>5,7,9-11</sup> Concerning the technical aspects, a large flip angle, a very short repetition time (TR), symmetrical and balanced gradient around the echo time (TE) and SSFP sequences could allow very fast imaging with a high signal to noise ratio (SNR).<sup>7,9-11</sup>

Tissues with large T2/T1 ratios such as fluid, blood and fat present very high signals with this imaging modality; therefore, SSFP sequences can easily identify cisternal portions of cranial nerves due to its excellent CSF to nerve contrast and high spatial resolution.<sup>5,7,9,10</sup> The total imaging time is quite shorter and cisternal parts of the cranial nerves are visualized more properly.<sup>7,9-11</sup>

DRIVE could be added at the end of a TSE echo train in order to accelerate the relaxation and dephase the protons for turning back to the equilibrium of the magnetization.<sup>8</sup> It was theoretically based upon a 3D-TSE sequence which pushes the residual transverse magnetization into the longitudinal axis by the help of recovery pulses.<sup>8,10</sup> DRIVE could do a strong T2 contrast to TSE sequences and CSF seems to be brighter.<sup>10</sup> The shortened TR helps to overcome the flow void artifacts, this further increases the bright-

ness of liquids, also shortens the imaging period with preserving high signals from fluids. DRIVE sequences also supply less available time for recovering magnetization at the end of a long echo train and the flow voids caused by CSF motion.<sup>8,10</sup>

To our experience, very few cases have been presented for visualization of the hypoglossal nerve with MR imaging before. Yousry et al.<sup>5</sup> identified the 12th cranial nerve as 82.5% (33 of 40) using the 3D-CISS sequence. They did not show the nerve exactly on T2W FSE sequences (0 of 40). The nerve was partially visualized in four cases with T2W FSE sequence. Their 3D-CISS results were higher than our ratios but their T2W FSE results were much lower than our findings.

Cheng et al.<sup>7</sup> studied 25 volunteers and succeeded in identifying the hypoglossal nerve as 66% using the 3D-FIESTA sequence, including the probably identified part as 52% and certainly identified part as 14%. With the 2D-FSE sequence, they could not identify any hypoglossal nerve. Except for the enhanced T1W series, our three sequences showed the 12th nerve much better than this research.

Hatipoglu et al.<sup>10</sup> presented a research with 50 patients using the 3D-FIESTA sequence. They succeeded as 91% in visualizing the hypoglossal nerve; 64% regularly identified, 27% partially identified, but with T2W FSE they only showed 2% of all nerves (one totally, one partially identified). Their 3D-FIESTA results were higher than our B-FFE and T2W 3D-DRIVE findings, but their incidental results of T2W FSE were far lower than our T2W TSE results.

Davagnam<sup>12</sup> studied hypoglossal nerves of 10 patients, undergoing routine follow-up imaging for vestibular schwannomas. Fischbach et al.<sup>13</sup> studied 12 healthy volunteers, applying T2W FSE and FRFSE sequences with 1.5 T and 3.0 T MRI systems.

Using contrast-enhanced 3D-FIESTA sequence, Davagnam<sup>12</sup> showed the nerve in all cases and concluded that 3D-FIESTA sequence with contrast is much more effective in identifying the lower cranial nerves. Fischbach et al.<sup>13</sup> showed 100% success rate in FSE and 25% success in FRFSE by the 1.5 T system. In the 3.0 T system with FSE the ratio increased to 40% and with FRFSE sequence the ratio elevated to 75%. Our results were much better and higher with correspondence to their T2W TSE and T2W DRIVE

sequences in the 1.5 T system.

To our knowledge, our research is probably the first paper in the literature that was fitted to analyze the best sequence in the depiction of the hypoglossal nerve and for this reason we performed these four sequences; namely, B-FFE, T2W DRIVE, T2W 2D-TSE and post contrast T1W sequences for all the patients. According to our experience, the least import visualization of the 12th cranial nerve belonged to the post-contrast T1W series, in which only 28 nerves were visualized (16 certainly, 12 probably identified) in our work. By application of T2W TSE DRIVE, 90 nerves were depicted, 60 nerves were certainly depicted and 30 were partially seen (scores 2 and 1, respectively).

In the T2W TSE sequence, 30 nerves were certainly depicted and 14 nerves were partially visualized (scores 2 and 1, respectively).

T2-DRIVE sequence was more beneficial than the T2W-TSE sequence in proper visualization of the cisternal segments of the hypoglossal nerve.

Using the B-FFE sequence, altogether 128 nerves (64%) were identified, of which 112 nerves were clearly depicted and 16 nerves were probably identified (scores 2 and 1, respectively). B-FFE sequence seemed to have more advantages in the visualization of hypoglossal nerves than the other sequences.

In conclusion, B-FFE, a SSFP gradient echo sequence with high spatial resolution, shorter imaging time with 1.0 mm slice thickness, 308×320 matrix, 50° flip angle, 2-3 number of excitation (NEX) is the optimized sequence for visualization of the cisternal part of the hypoglossal nerve. In our study, there was a 64% success rate in determining the hypoglossal nerve (56% regularly, 8% partially identified). This sequence enables more advantages in visualizing the 12th cranial nerve among other sequences.

T2W-DRIVE is the second sequence and more diagnostic than the T2W TSE images. DRIVE sequence is far more important in determining the 12th cranial nerve than the post-contrast T1W series and T2W TSE sequences. The post-contrast T1W series has the least importance in the depiction of the hypoglossal nerve, so contrast agent application has only limited

value.

## Acknowledgements

We are very thankful to Mr. Haydar Polat and Mr. Egemen Alper for their willingness in managing the figures, we also thank Mr. Sükrü Yılmaz for his brief help in processing all the images and writing the paper.

## References

1. Laine FJ, Underhill T. Imaging of the lower cranial nerves. *Neuroimaging Clin N Am* 2004 Nov;14(4):595-609.
2. Gibo H, Marinkovic S, Nikodijevic I, Stimec B, Erden A. The blood supply of the hypoglossal nerve: the microsurgical anatomy of its cisternal segment. *Surg Neurol* 1997;48(1):85-91.
3. Smoker WRK. The hypoglossal nerve. *Neuroimaging Clin N Am* 1993;3:193-206.
4. Harnsberger HR. The lower cranial nerves (7-12). In: Osborn AG, Bragg DG, editors. *Handbooks in radiology: Head and neck imaging*. Chicago: Year book Medical Publishers; 1995. p. 488-521.
5. Yousry I, Camelio S, Schmid U.D, Horsfield MA, Wiesmann M, Brückmann H et al. Visualization of cranial nerves 1-12: Value of 3D-CISS and T2-weighted FSE sequences. *Eur Radiol* 2000;10(7):1061-7.
6. Yousry I, Moriggl B, Dieterich M, Naidich TP, Schmid UD, Yousry TA. MR anatomy of the proximal cisternal segment of the trochlear nerve: neurovascular relationships and landmarks. *Radiology* 2002;223(1):31-8.
7. Yu Shu C, Zheng-rong Z, Wei-jun P, Feng T. Three-dimensional fast imaging employing steady-state acquisition and T2-weighted fast-spin echo magnetic resonance sequences on visualization of cranial nerves 3-12. *Chin Med J* 2008;121(3):276-9.
8. Ciftci E, Anik Y, Arslan A, Akansel G, Sarisoy T, Demirci A. Driven equilibrium (drive) MR imaging of the cranial nerves 5-8: comparison with the T2-weighted 3D TSE sequence. *Eur J Radiol* 2004;51(3):234-40.
9. Tsuchiya K, Aoki C, Hachiya J. Evaluation of MR cisternography of the cerebellopontine angle using a balanced fast-field-echo sequence: preliminary findings. *Eur Radiol* 2004;14(2):239-42.
10. Hatipoglu H.G, Durakoglugil T, Ciliz D, Yuksel E. Comparison of FSE T2W and FIESTA sequences in the evaluation of posterior fossa cranial nerves with MR cisternography. *Diagn Interv Radiol* 2007;13(2):56-60.
11. Mikami T, Minamida Y, Yamaki T, Koyanagi I, Nonaka T, Houkin K. Cranial nerve assessment in posterior fossa tumours with fast imaging employing steady-state acquisition (FIESTA). *Neurosurg Rev* 2005;28(4):261-6.
12. Davagnanam I, Chavda SV. Identification of the normal jugular foramen and lower cranial nerve anatomy: Contrast-enhanced 3D Fast Imaging Employing Steady-State Acquisition MR imaging. *AJNR Am J Neuroradiol* 2008;29(3):574-6.
13. Fischbach F, Muller M, Bruhn H. Magnetic resonance Imaging of the cranial nerves in the posterior Fossa: a comparative Study of T2-Weighted Spin echo Sequences at 1.5 T and 3.0 T. *Acta Radiol* 2008;49(3):358-63.